COBEM 2023 27TH INTERNATIONAL CONGRESS OF MECHANICAL ENGENEERING

ABCM Brazilian Society of Mechanical Sciences and Engineering
27th ABCM International Congress of Mechanical Engineering
December 04-08, 2023, Florianópolis-SC, Brazil

COB-2023-2397
TEMPORAL EVOLUTION OF RESUSPENTION POTENTIAL AROUND SUCCESSIVE STOCKPILES USING THE OIL-FILM TECHNIQUE

Cristina Lima de Morais
Bruno Furieri
Jane Meri Santos
Federal University of Espírito Santo, Department of Environmental Engineering, 29075-910, Vitória, ES, Brasil.
cristinalimademorais@gmail.com, bruno.furieri@ufes.br, jane.m.santos@ufes.br

Jean-Luc Harion
IMT Nord Europe, 59500, Douai, França.
jean-luc.harion@imt-nord-europe.fr

Abstract. *Open industrial yards are used to store large amounts of granular material such as coal, iron ore and limestone, for instance. Due the erosion caused by wind, these materials can be emitted to the atmosphere offering risks to the environment and to the human health. To select dust control techniques and comply with environmental polices requirements, it is important to understand the disturbance to atmospheric flow caused by the presence of the stockpiles and to estimate the particles emission to the atmosphere due to wind erosion. There are several studies on particles emission from stockpiles surfaces, but only few studies considering the emission that may occur from the regions that surround the stockpiles. In these regions, emission can occur from ground soil or can be originated from the transport of material within the industrial site as from the erosion of the stockpiles, charactering a re-emission event. The present work aims to investigate the temporal evolution of the resuspension potential around successive stockpiles using the oil-film technique. Laboratory experimental simulations of the wind flow over two successive wood stockpiles models oriented 30°, 60° and 90° to the incoming flow were performed. Photographs were taken during the experiment and the temporal evolution of the shear stress patterns on the ground surface were evaluated. The results show that the regions on the ground surface surrounding the two piles oriented at 90° presented lower levels of shear stress whilst the same regions surrounding the two piles oriented at 60° gave higher levels of shear stress. Regions on the ground surface around the two piles oriented at 30° to the incoming flow represent the intermediate case among those studied regarding the level of shear stress. Furthermore, the regions around piles oriented at 30 and 60° reach the final stage of the oil-film pattern modification faster, indicating that the stockpiles orientation (or wind direction) has a strong influence on the erosion potential.*

Keywords: *open yards, wind erosion, particulate matter, stockpiles, oil-film technique.*

1. INTRODUCTION

Particulate matter of very smaller diameter at high concentrations in atmospheric air can negatively impact the environment, human beings and how they relate to each other (Huang et al., 2009; Wu et al., 2005; Tiwary and Colls, 2010; An et al., 2018; Bové et al., 2019; Hadley et al., 2018; Miller, 2020; Novak et al., 2015; Seaton et al., 2020; Sigaux et al., 2019). The steel industry plays an important role in dust emission, since they maintain particulate matter stored in piles in their open yards. Such materials, as iron ore, coal and limestone, for instance, are used in steel production and can be easily carried out by the wind depending on meteorological conditions. Many efforts have been made to improve the estimation of emission from stockpiles surfaces (Badr, 2007; Badr and Harion, 2007, 2005; Derakhshani et al., 2013; Diego et al., 2009; Faria et al., 2011; Farimani et al., 2011; Toraño et al., 2007; Turpin and Harion, 2009; de Morais et al., 2018; Ferreira et al., 2020), however, there is much more to be notice in an open industrial yard. Particles can be dropped into regions around the piles by operations of addition or material removal. Trucks may drop material during transport and so on. The dynamics of industrial yards are so strong that one cannot predict exactly where the particles might come from, but one can guarantee that they exist in regions outside the surface of the pile, and they can be emitted. This emission characterizes a re-emission or resuspension event.

Furieri *et al*. (2012) studied the flow field around an isolated stockpile using the oil-film technique to understand the flow features that may lead to emission of particles that have settled in the surroundings of a stockpiles, evaluating the flow topology for three different wind directions. Furieri et al. (2014) performed numerical simulations in order to quantify the emitted particles from the surroundings areas and evaluate numerically the shear stress distribution. In the present work, we take a step forward to complement the analysis of resuspension events around stockpiles employing the oil-film technique to assess the evolution of erosion potential over the time.

2. BRIEF WALL FLOW VISUALIZATION STATE OF THE ART

The perception of a physical phenomenon is always improved when the pattern produced by or related to that physical phenomenon can be visualized. This is specifically relevant in the case where fluids are investigated, because through the visualization it is possible to have an idea of the structures present in the flow and its development. The previous knowledge of the flow structure is very important as a reference for the development of theories, measurements and simulations. In addition, visualization can also help in choosing the appropriate technique for measuring magnitudes of the phenomenon related to the flow.

For all type of fluid flow, the visualization is an important tool in experimental fluid mechanics, which can provide a general view of the flow field. Experimental flow visualization techniques are applied to get an image of fluid flow around a model, without any calculations and, for develop or verify theories of fluid flow. Flow visualization can be divided into (i) surface flow visualization and (ii) off-the-surface visualization. The first one, uses tufts, fluorescent dye, oil or special clay mixtures, which are applied to the surface of a model. Visual inspection of such tufts and coatings as a function of time or after some time, may give valuable information on fluid patterns, wake zones and state of the boundary layer. The second type of visualization uses tracers as smoke particles, oil droplets or helium-filled soap bubbles. Each of these methods requires appropriate lighting and some device for recording the image such as a still or video camera. (Ristić and Eng, 2007; Örlü and Vinuesa, 2020).

According to Lu (2010) and Zhang et al. (2019), surface flow visualization can also provide an initial indication of complex flow structures. In other words, it indicates that a potentially complex flow exists so that more elaborate techniques should be used. Besides, the visualization provides qualitative information about the flow itself, although the interpretation of the visualization may be difficult, requiring some skill and experience. Topological rules are necessary for tying the footprint to the rest of the flow. Instantaneous topologies of unsteady flows, for instance, require time solved data and are similarly described. However, surface flow visualization, which depends on the motion of a thin liquid layer, is not able to track unsteadiness. The two major forms of unsteadiness are turbulence and gross time dependency such as periodic motions or, due to shock/boundary layer interactions (Lu, 2010; Zhang et al., 2019).

Recently, many authors have been working in order to improve the oil-film techinique. Azetsu et al. (2019) proposed a new method for oil-film visualization for transport process of lubricant oil around an engine piston. They dissolved a photochromic dye in the oil and an arbitrary spot of an oil film was illuminated with ultraviolet light, which makes a marker in the oil film via a photochromic reaction. The color density of the colored solution is quantified based on the absorbance calculated from images taken before and after coloring. The results confirm that the color density is proportional to the oil film thickness. Zhang et al. (2019) investigated the flow over model of a complex cambered, twisted, tapered wing with 40° leading edge sweep. The experiments investigated the flow using the oil-film visualization, stereo particle image velocimetry and force moment measurements. Still images combined with video clips enable flow patterns over the wing model to be interpreted more clearly and accurately. The flow topology was correlated with the aerodynamic forces and moments to illustrate how the flow structures affect the performance of the swept wing. He et al. (2021) studied the complex flow structure of a high-speed cavity through a single-color fluorescent oil flow visualization system in the wind tunnel of China Aerodynamic Research Development Centre in order to improve the system. Different parts of cavity were evaluated with different oil films with different fluorescent particles to visualize the flow mixing more effectively. Additionally, specialized ultraviolet light sources were used to enhance the oil flow image contrast. To assure that the oil-film correctly follows the flow, the thickness and viscosity of the oil film were controlled. The experimental result showed that the improved oil flow system can effectively visualize complex flow patterns of the cavity even mixing flows.

3. RESUSPENTIALPOTENTIAL

The evaluation of resuspension potential around stockpiles came from the emission model proposed by the United States Environmental Protection Agency (USEPA, 2006). This methodology uses the concept of erosion potential, estimated by:

$$P = 58(u_* - u_{*t})^2 + 25(u_* - u_{*t}) \quad (1)$$

where P is the erosion potential [g/m²], u_* is the friction velocity [m/s] and u_{*t} is the threshold friction velocity [m/s].

In general words, the balance between u_* and u_{*t} defines if some region composed by granular material will emit particles or not. The friction velocity is a conceptual representation of the shear stress ($u^* = \sqrt{\tau/\rho}$, where τ is the wind shear stress and ρ the air density) and is related with the forces that act to move particles in an erosion event, as drag and lift forces. The threshold friction velocity is the friction velocity at which the particles initiate its movement and depend on its properties as diameter, density, moisture, etc. This variable is related to the forces that act to avoid the particle movement, as gravity and cohesion forces. The threshold friction velocity can be measured in wind tunnels and even

estimated (Foucaut & Stanislas, 1996; Iversen & White, 1982; Shao & Lu, 2000). If $u_* < u_{*t}$, the region does not have potential do emit particles. Otherwise, if $u_* > u_{*t}$, the region has potential do emit particles.

Suspension or resuspension potential can be evaluated quantitatively by Equation 1. However, as previously mentioned, the present work concerns to qualitatively evaluate the erosion potential by changes in the wall flow patterns through the oil-film technique. The changes in the oil-film coloration during the wind flow will indicate the level of shear stress faced by the wall region around the successive stockpiles.

4. EXPERIMENTAL WORK

The oil-film used to perform the experiments was composed by 128 g/m² of paraffin oil, 5 g/m² of yellow dye and 23 drops/m² of oleic acid (Figure 1). The paraffin oil represents the oil part and the oleic acid represent the mixing agent (Desreumaux and Bourez 1989). The stockpiles models, made by wood, were placed in the test section of the wind tunnel showed in Figure 2. All flow requirements to simulate a full developed turbulent boundary layer were reached. Details can be found in Furieri et al. (2012b) and Ferreira et al. (2020). Above the test section was placed a photographic camera in order to record the oil-film movement according to wind shear stress. For all tested cases, the free stream velocity of 6.5 m/s was chosen. Table 1 presents the studied cases.

Figure 1. Three compounds used in the oil-film mixture: (a) paraffin oil, (b) yellow powder and (c) oleic acid.

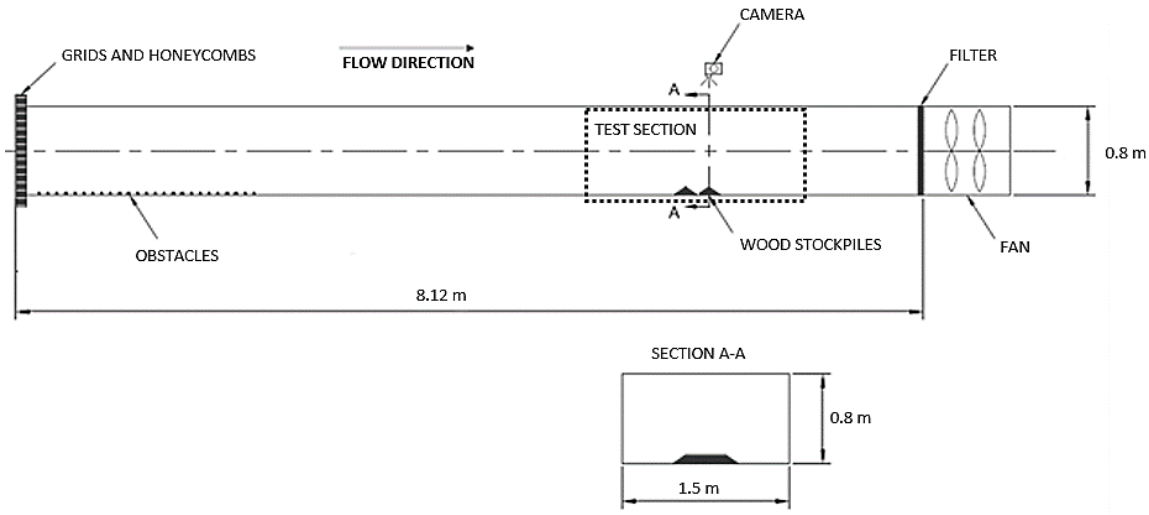

Figure 2. Schema of wind-tunnel used in the oil-film experiment. Adapted from Ferreira et al. (2020).

Table 1. Experimental configurations investigated.

Stockpiles characteristics	Wind direction	Gap[(1)]
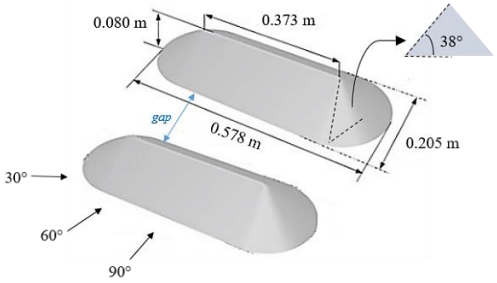	30°	1e
	60°	2e
	90°	2e

(1) 0.9h, where h is the stockpile height of 0.080 m

5. WALL FLOW STRUCTRURES TEMPORAL EVOLUTION

The region chosen to be coated in the wind-tunnel is that enough to visualize all the wall flow structures around the pile, for instance, for a perpendicular stockpile: 5.0 cm (approximately 0.25l) upstream to the visualization of the windward wall, stagnation zone and flow acceleration, 83.0 cm (approximately 4.1l) downstream due to the necessity to visualize the wake zone and reattachment point and 20.0 cm (approximately 1l) on each side of the stockpile to visualize the formation of the main vortices and the flow acceleration effects on the laterals. l is the stockpile length represented in Figure 3. It is also possible to observe in Figure 3 that regions of intense dark color are regions that face high levels of shear stress. On the other hand, regions with intense yellow color represents face the opposite.

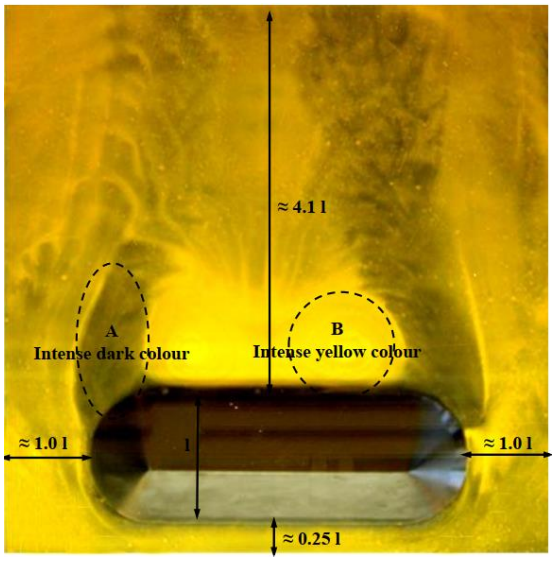

Figure 3. Typical photograph of oil-film surface flow visualization.

Figure 4 presents the temporal evolution of the resuspension potential for the incoming wind flow of 30° every one hour. At the beginning (Figure 4a), the wall surface is mainly yellow, indicating that the phenomenon has already started. Over the time (Figure 4b, 4c and 4d), it is possible to see the flow patterns formed by the shear stress according to the stockpiles and wind configuration. Regions of intense dark color show where the erosion potential is greatest as well as the friction velocity. Depending on the material that could be there, probably be the emission of particulate matter would occur.

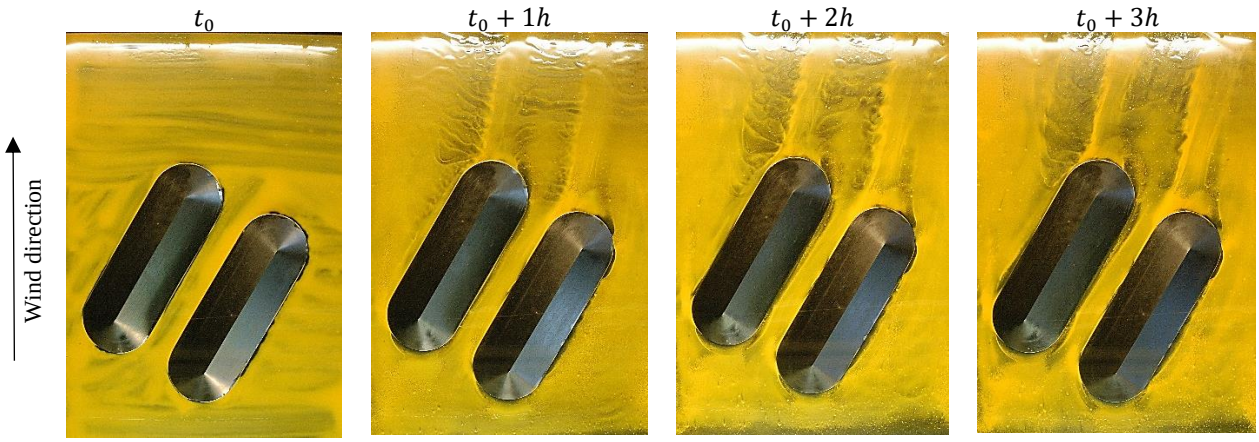

Figure 4. Oil-film visualization around successive stockpiles oriented 30° to the incoming flow.

The same discussion can be applied for temporal evolution of the suspension potential for the incoming wind flow of 60° and 90° as can be seen in Figure 5 and Figure 6. The difference remains in the flow patterns developed and in the intensity of the shear stress presented in these cases. The contours for the 60° case are well outlined and present intense dark color. The contours of 90° case are smoother, and the shear level is less intense as well as lighter yellow color. Evaluating the temporal evolution, when the piles are orientated at 60° to the incoming flow, the final state of the oil-film pattern are reached faster than the other cases.

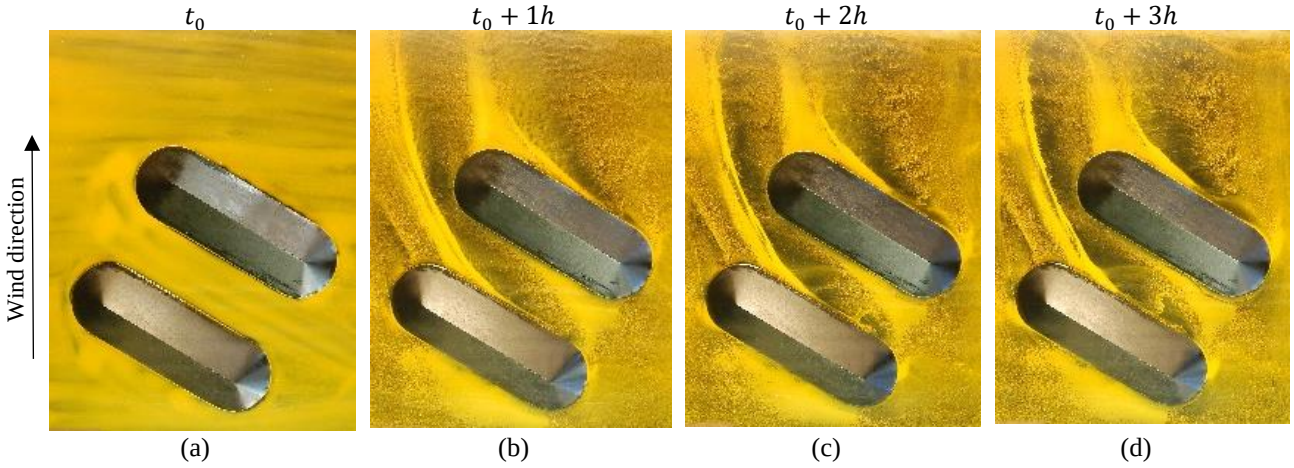

Figure 5. Oil-film visualization around successive stockpiles oriented 60° to the incoming flow.

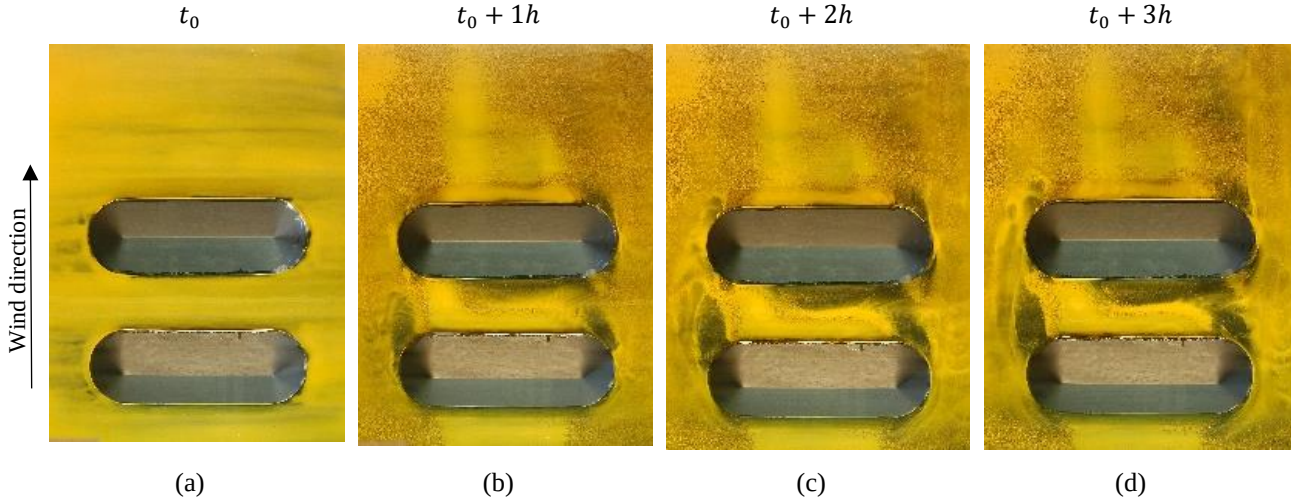

Figure 6. Oil-film visualization around successive stockpiles oriented 90° to the incoming flow.

6. CONCLUSION

The resuspension potential around successive stockpile was evaluated over the time using the oil-film technique. The results show that the regions on the ground surface surrounding two piles oriented at 90° to the incoming flow presented lower levels of shear stress whilst the same regions surrounding the two piles oriented at 60° gave higher levels of shear stress. Regions on the ground surface around the two piles oriented at 30° to the incoming flow represent the intermediate case among those studied regarding the level of shear stress. Furthermore, the regions around piles oriented at 30 and 60° reach the final stage of the oil-film pattern modification faster, indicating that the stockpiles orientation (or wind direction) has a strong influence on the erosion potential.

7. ACKNOWLEDGEMENTS

This study was financed in part by the Coordenação de Aperfeiçoamento de Pessoal de Nível Superior - Brasil (CAPES) - Finance Code 001. It was also carried out with the financial support of Fapes (Fundação de Amparo à Pesquisa e Inovação do Espírito Santo), ArcelorMittal and EDF R&D.

8. REFERENCES

An, Z., Jin, Y., Li, J., Li, W., & Wu, W. (2018). Particulate Matter. *Current Allergy and Asthma Reports*, *18*(15), 3–9. https://doi.org/https://doi.org/10.1007/s11882-018-0768-8

Azetsu, A., Kitajima, I., & Kuratsuji, K. (2019). Development of a new visualization technique using photochromism for transport process of lubricating oil around the engine piston. *International Journal of Engine Research*, *20*(7), 777–787. https://doi.org/10.1177/1468087418819229

Badr, T. (2007). *Quantification des émissions atmosphériques diffuses produites par érosion éolienne*.

Badr, T., & Harion, J. L. (2005). Numerical modelling of flow over stockpiles: Implications on dust emissions. *Atmospheric Environment*, *39*(30), 5576–5584. https://doi.org/10.1016/j.atmosenv.2005.05.053

Badr, T., & Harion, J.-L. (2007). Quantification of diffuse dust emissions from open air sources on industrial sites. *3rd IASME/WSEAS International Conference on Energy, Environment and Sustainable Development (EEESD '07), ISBN: 978-960-8457-88-1*, *January*, 276–280.

Bové, H., Bongaerts, E., Slenders, E., Bijnens, E. M., Saenen, N. D., Gyselaers, W., Van Eyken, P., Plusquin, M., Roeffaers, M. B. J., Ameloot, M., & Nawrot, T. S. (2019). Ambient black carbon particles reach the fetal side of human placenta. *Nature Communications*, *10*(1), 1–7. https://doi.org/10.1038/s41467-019-11654-3

De Morais, C. L., Ferreira, M. C. S., Santos, J. M., Furieri, B., & Harion, J. L. (2018). Influence of non-erodible particles with multimodal size distribution on aeolian erosion of storage piles of granular materials. *Environmental Fluid Mechanics*, *0123456789*. https://doi.org/10.1007/s10652-018-9640-6

Derakhshani, S. M., Schott, D. L., & Lodewijks, G. (2013). Dust emission modelling around a stockpile by using computational fluid dynamics and discrete element method. *AIP Conference Proceedings*, *1542*, 1055–1058. https://doi.org/10.1063/1.4812116

Desreumaux, O., & Bourez, J. P. (1989). *Préparation de bouillies pour visualisation pariétales sur maquette de sous-marin à cepra 19*.

Diego, I., Pelegry, A., Torno, S., Toraño, J., & Menendez, M. (2009). Simultaneous CFD evaluation of wind flow and dust emission in open storage piles. *Applied Mathematical Modelling*, *33*(7), 3197–3207. https://doi.org/10.1016/j.apm.2008.10.037

Faria, R., Ferreira, A. D., Sismeiro, J. L., Mendes, J. C. F., & Sousa, A. C. M. (2011). Wind tunnel and computational study of the stoss slope effect on the aeolian erosion of transverse sand dunes. *Aeolian Research*, *3*(3), 303–314. https://doi.org/10.1016/j.aeolia.2011.07.004

Farimani, A. B., Ferreira, A. D., & Sousa, A. C. M. (2011). Computational modeling of the wind erosion on a sinusoidal pile using a moving boundary method. *Geomorphology*, *130*(3–4), 299–311. https://doi.org/10.1016/j.geomorph.2011.04.012

Ferreira, M. C. S., Furieri, B., de Morais, C. L., Stocco, J. F., Reis Jr, N. C., Harion, J.-L., & Santos, J. M. (2020). Experimental and numerical investigation of building effects on wind erosion of a granular material stockpile. *Environmental Science and Pollution Research*, *27*, 14.

Foucaut, J. M., & Stanislas, M. (1996). Take-off threshold velocity of solid particles lying under a turbulent boundary layer. *Experiments in Fluids*, *20*(5), 377–382. https://doi.org/10.1007/BF00191019

Furieri, B., Russeil, S., Harion, J. L., Turpin, C., & Santos, J. M. (2012). Experimental surface flow visualization and numerical investigation of flow structure around an oblong stockpile. *Environmental Fluid Mechanics*, *12*(6), 533–553. https://doi.org/10.1007/s10652-012-9249-0

Furieri, B., Russeil, S., Harion, J., Santos, J., & Milliez, M. (2012). Comparative analysis of dust emissions : isolated stockpile vs two nearby stockpile. *WIT Transactions on Ecology and The Environment*, *157*, 285–293. https://doi.org/10.2495/AIR120

Furieri, B., Santos, J. M., Russeil, S., & Harion, J. L. (2014). Aeolian erosion of storage piles yards: Contribution of the surrounding areas. *Environmental Fluid Mechanics*, *14*(1), 51–67. https://doi.org/10.1007/s10652-013-9293-4

Hadley, M. B., Vedanthan, R., & Fuster, V. (2018). Air pollution and cardiovascular disease: A window of opportunity. *Nature Reviews Cardiology*, *15*(4), 193–194. https://doi.org/10.1038/nrcardio.2017.207

He, B., Li, G., Zhou, F., Liu, D., & Xiang, X. (2021). Application of colour fluorescent oil flow visualization for a high speed cavity. *Journal of Physics: Conference Series*, *1786*(1). https://doi.org/10.1088/1742-6596/1786/1/012049

Huang, W., Tan, J., Kan, H., Zhao, N., Song, W., Song, G., Chen, G., Jiang, L., Jiang, C., Chen, R., & Chen, B. (2009). Visibility, air quality and daily mortality in Shanghai, China. *Science of the Total Environment*, *407*, 3295–3300.

Iversen, J. D., & White, B. R. (1982). Saltation threshold on Earth, Mars and Venus. *Sedimentology*, *29*, 111–119.

Lu, F. K. (2010). Surface oil flow visualization. In *European Physical Journal: Special Topics* (Vol. 182, Issue 1, pp. 51–63). https://doi.org/10.1140/epjst/e2010-01225-0

Miller, M. R. (2020). Oxidative stress and the cardiovascular effects of air pollution. *Free Radical Biology and Medicine*, *November 2019*. https://doi.org/10.1016/j.freeradbiomed.2020.01.004

Novak, L., Bizjan, B., Pražnikar, J., Horvat, B., Orbanić, A., & Širok, B. (2015). Numerical Modeling of Dust Lifting from a Complex-Geometry Industrial Stockpile. *Strojniski Vestnik/Journal of Mechanical Engineering*, *61*(11), 621–631. https://doi.org/10.5545/sv-jme.2015.2824

Ristić, S., & Eng, (2007). Flow Visualisation Techniques in Wind Tunnels Part I-Non optical Methods. In *Scientific Technical Review: Vol. LVII* (Issue 1). https://www.researchgate.net/publication/267296233

Seaton, Tran, Chen, Maynard, & Whalley. (2020). Pollution, Particles, and Dementia: A Hypothetical Causative Pathway. *International Journal of Environmental Research and Public Health*, *17*(3), 862. https://doi.org/10.3390/ijerph17030862

Shao, Y., & Lu, H. (2000). A simple expression for wind erosion threshold friction velocity. *Journal of Geophysical Research*, *105*, 22437–22443. https://doi.org/https://doi.org/10.1029/2000JD900304

Sigaux, J., Biton, J., André, E., Semerano, L., & Boissier, M. C. (2019). Air pollution as a determinant of rheumatoid arthritis. *Joint Bone Spine*, *86*(1), 37–42. https://doi.org/10.1016/j.jbspin.2018.03.001

Tiwary, A., & Colls, J. (2010). Air pollution: measurement, modelling and mitigation. In *Choice Reviews Online* (3rd ed., Vol. 47, Issue 08). Routledge Taylor and Francis Group. https://doi.org/10.5860/choice.47-4447

Toraño, J. A., Rodriguez, R., Diego, I., Rivas, J. M., & Pelegry, A. (2007). Influence of the pile shape on wind erosion CFD emission simulation. *Applied Mathematical Modelling*, *31*(11), 2487–2502. https://doi.org/10.1016/j.apm.2006.10.012

Turpin, C., & Harion, J. L. (2009). Numerical modeling of flow structures over various flat-topped stockpiles height: Implications on dust emissions. *Atmospheric Environment*, *43*(35), 5579–5587. https://doi.org/10.1016/j.atmosenv.2009.07.047

USEPA. (2006). 13.2.5 Industrial wind erosion. *Compil Air Pollut Emiss Factors*, *1*. https://doi.org/10.1130/0091-7613(1998)026<0363

Wu, D., Tie, X., Chengcai, L., Zhuming, Y., Lau, A. K. H., & Huang, J. (2005). An extremely low visibility event over Guangzhou region: a study case. *Atmospheric Environment*, *39*, 6568–6577.

Zhang, S., Jaworski, A. J., McParlin, S. C., & Turner, J. T. (2019). Experimental investigation of the flow structures over a 40° swept wing. *Aeronautical Journal*, *123*(1259), 39–55. https://doi.org/10.1017/aer.2018.118

9. RESPONSIBILITY NOTICE

The authors are the only responsible for the printed material included in this paper.